

STUDY OF THE DEPENDENCE OF FREQUENCY UPON MICROWAVE
POWER OF WALL-COATED AND BUFFER-GAS-FILLED PASSIVE
Rb⁸⁷ FREQUENCY STANDARDS

A. Risley and Stephen Jarvis, Jr.
(National Bureau of Standards, Boulder, Colorado)

and

J. Vanier, (Université Laval, Quebec, Canada)

Summary

Previous studies of a commercial passive gas cell Rb⁸⁷ frequency standard showed a strong dependence of the output frequency, ν_{Rb} , upon the microwave power, $P_{\mu\lambda}$. A major conclusion of that work was that the dependence of ν_{Rb} upon $P_{\mu\lambda}$ was due to a line inhomogeneity effect. The line inhomogeneity interpretation suggested that substituting a wall coating for the usual buffer gas would reduce the dependence upon $P_{\mu\lambda}$. As a part of the present work a wall coating (a form of paraffin) was used and a reduction of this dependence by a factor of 100 was obtained.

The present work has led to a more convincing theoretical demonstration of the line inhomogeneity effect. The paper discusses some of the details of the analytical procedure.

There are certain major requirements that a wall coating would have to satisfy if it were to be superior to the usual buffer gas and these are discussed in the text. The advantages demonstrated by the present work indicate that further studies are warranted to determine if an improved standard could be built based on a wall coating.

Background

The passive Rb⁸⁷ gas cell frequency standard is the most prevalent type of atomic frequency standard in the field. It gives good performance at a fairly low cost. The results of the work reported here suggest that the use of a wall coating instead of the usual buffer gas might improve its medium and long term frequency stability.

Earlier work on a prevalent commercial Rb⁸⁷ standard demonstrated a very strong frequency dependence upon the microwave power, $P_{\mu\lambda}$.¹ This effect appears to be due to a combination of relatively immobile Rb⁸⁷ atoms and a frequency gradient across the absorption cell. The immobility is due to the use of a buffer gas in the cell.

The work reported here demonstrated that a strong signal can be obtained by substituting a wall coating for the buffer gas. Making this substitution results in a drastically reduced dependence of the output frequency, ν_{Rb} , upon $P_{\mu\lambda}$. In the commercial unit studied in reference 1, the dependence upon $P_{\mu\lambda}$ caused by the line inhomogeneity was probably the predominant cause of fre-

quency instability for averaging times of the order of one month and longer. Thus, the ability to use wall coating in lieu of buffer gas might be important commercially.

In section II we discuss the experimental results of the present work. Section III gives the results of the line inhomogeneity analysis which represents our understanding of the dependence of ν_{Rb} upon $P_{\mu\lambda}$ when a buffer-gas is used. In section IV we discuss some pros and cons of using wall coatings.

Experimental Results

Experimental Setup

The experimental arrangement used in these experiments is shown in figure 1. An optical package capable of giving a strong resonance of the $F = 2, M_F = 0$ to $F = 1, M_F = 0$ transition was used to lock the frequency of a crystal oscillator driving a frequency synthesizer. The frequency was measured then with a counter. The arrangement gave a resolution of 1×10^{-10} which was sufficient for the types of phenomena studied. The optical package--consisting of a rubidium 87 lamp, an isotopic filter, and a TE₀₁₁ exciting cavity--was equipped with a special cell. This cell, made of quartz, was coated with a form of paraffin and connected to a vacuum system. It contained a few milligrams of rubidium 87 in a tail, whose temperature could be controlled independently of the cavity. In our work a typical tail temperature was 70° C. The cell was 3.2 cm in diameter and typically was held at 71° C. The cavity was 5.7 cm in diameter and about 7 cm long. (In the unit studied in reference 1, the cell filled the entire cavity.)

It is important to say that the experimental arrangement was considerably different (and more controlled) here than in reference 1. Nevertheless, our earlier conclusion about line inhomogeneity as the mechanism producing the dependence upon $P_{\mu\lambda}$ is strongly supported by the present work. An additional aspect of the present work was that the Q of the cavity was sufficiently high that a cavity pulling effect could be observed although the system was operated in the passive mode. These results will be reported elsewhere.²

In order to study the effects of power shift in the presence of frequency gradients across the cell, special coils were mounted at the end of the cavity. These coils were about 4.5 cm in diameter and were separated by 7 cm. Each consisted of 150 turns. The coils could produce a magnetic field

gradient which was then translated by the rubidium 87 atomic ensemble to a frequency gradient.

The effect of gradients of this sort could then be studied under controlled conditions, and in circumstances where the atom was free to average the magnetic gradient and light shift in the case of the coated cells, or where the atoms were fixed in space with a buffer gas. In this last case, the field gradients and light shift are not averaged by the atomic motion and inhomogeneous broadening and shifting of the resonance line occurs. This shifting and broadening depends on the level of $P_{\mu\lambda}$ and, thus, the frequency dependence upon $P_{\mu\lambda}$ results.

Results

ν_{Rb} versus $P_{\mu\lambda}$ and Magnetic Gradient. Figure 2 shows ν_{Rb} versus $P_{\mu\lambda}$, with the voltage applied to the gradient coils as a parameter. The level of $P_{\mu\lambda}$ is determined by the microwave attenuator and, for an attenuator setting of 50 dB, the power absorbed by the cavity is approximately 1×10^{-10} watts. The data of figures 2 through 5 were taken with the cavity frequency no more than 25 kHz away from ν_{Rb} . Based on our cavity pulling measurements, we conclude that the worst case pulling of ν_{Rb} would be no more than 0.25 Hz due to this offset. Since the precision of the frequency measurements is about 0.7 Hz, cavity pulling effects are negligible.

The resonant frequency of any given atom has a quadratic dependence upon the magnetic field and the coils produce a linear field gradient across the cell. For the maximum voltage (1.6 volts) applied to the gradient coils, the resonant frequencies of the atoms vary across the cell by about 2,500 Hz. This is, of course, a much larger gradient than would be encountered in a working standard. The purpose in applying such a large gradient was twofold. First--since the spatial variation of the magnetic gradient is more accurately known than that of the light shift--we wanted to have a condition where the total gradient was primarily due to the magnetic gradient. Second, we wanted to clearly show the dramatic change in sensitivity to $P_{\mu\lambda}$ when the buffer gas is removed.

On the other hand, for applied gradient voltages less than about 0.2 volts, the light shift gradient dominates.

In figure 3 we have plotted the data in a different form. On the right ordinate scale, to emphasize the change in frequency with change in power, we have plotted a frequency change due to a 20 dB change in $P_{\mu\lambda}$ versus the gradient voltage.

The microwave change is from an attenuator setting of 40 dB to one of 20 dB. (As a point of further information, the maximum signal level at the lock-in amplifier occurs for a microwave attenuator setting of about 35 dB. The 100 Hz modulation voltage [see figure 1] used in all these measurements is one that produces a maximum signal level at the lock-in when the frequency of the microwave source is just slightly displaced from ν_{Rb} . [This is an open loop test.] This is a way of assuring that the microwave source is not being overmodulated.) This change in $P_{\mu\lambda}$ is, of course, vastly

larger than would be encountered in a commercial unit, and our purpose was to emphasize the difference between a buffer gas filled cell and one with only a wall coating. Also shown in figure 3 on the left ordinate is the resonant frequency as a function of applied gradient voltage at a 50 dB attenuation setting for the microwave power.

Figures 4 and 5 give the same information for the paraffin-coated unsealed cell attached to the vacuum system. For applied gradient voltages of 0.8 volts and less, there is no $P_{\mu\lambda}$ dependence to within the precision of the measurement.

The larger dependence of ν_{Rb} upon changes in $P_{\mu\lambda}$ shown in figures 2 and 3 should be contrasted with figures 4 and 5. Note also, the very different character of the center frequency, ν_{Rb} , in figure 3, as compared to figure 5. To understand this difference in the behavior of ν_{Rb} versus magnetic gradient (for fixed $P_{\mu\lambda}$), some additional information is needed.

First, the portion of the cell which is nearest the light source (the "input end" of the cell), is very near the center of the cavity so that the microwave field intensity, β , is near its maximum there. At the $P_{\mu\lambda} = 50$ dB level, and in this region, $P_{\mu\lambda}$ is just about at its optimum level for inducing transitions. Thus, for smaller attenuator settings, this region is in microwave saturation to a greater or lesser degree. Second, the magnetic field due to the gradient coils has a null just at the "input end" of the cell and so any atom's hyperfine frequency is the higher the further into the cell it finds itself.

Now, the response at the photocell is a weighted average of the absorption throughout the cell. For $P_{\mu\lambda} = 50$ dB, the major contribution is near the input end of the cell and this group of atoms experiences a weaker field (and, thus, a lower frequency) than the average field experienced by atoms that are free to move in the cell. If the theoretical results for ν_{Rb} --at $P_{\mu\lambda} = 50$ dB--are displayed as in figure 3, then a large decrease in slope at increasing values of V_g is also observed.

If a large value of $P_{\mu\lambda}$ ($P_{\mu\lambda} = 20$ dB) is used in the calculation, then a larger initial slope is obtained and this slope is roughly independent of V_g . This behavior is qualitatively consistent with the idea that a larger value of $P_{\mu\lambda}$ would increase the weighting of atoms nearer the center of the cell. But a person might expect that, for a fixed value of $P_{\mu\lambda}$, the weighting would be fixed, i.e., independent of V_g . However, for large values of V_g , the frequency change over even a small segment of the cell near the output end is large compared to the low-power, non-homogeneity broadened linewidth (see section II.B.2). This means that the number of atoms available for microwave absorption--per unit bandwidth of the microwave source--is severely decreased near the output end of the cell. Thus--for a fixed value of $P_{\mu\lambda}$ --the resonant frequency of all atoms in the cell

risers with increasing V_g , but those segments of the cell for which it rises the most become increasingly less effective at determining the center frequency. This causes the weighting to be shifted toward the front of the cell as V_g increases. A comparison with data (not shown here) for larger values of $P_{\mu\lambda}$ gives the same qualitative behavior as for the theory. Moreover, even in the worst case, the ratio of the theoretical to the experimental value is less than 2.

Linewidth versus $P_{\mu\lambda}$ and Pumping--Light Intensity.

At the $P_{\mu\lambda} = 20$ dB level--which is 15 to 20 dB higher than that which produces the maximum signal (with the low modulation level that was used)--microwave power broadening is responsible for about 60 percent of the linewidth.

If the magnetic gradient is turned off and $P_{\mu\lambda}$, I_0 (the pumping--light intensity), and the modulation voltage reduced to as low a value as possible for obtaining a usable signal (about a factor of 4 lower than was typical for I_0 and the modulation voltage), then the linewidth, $\Delta\nu_{Rb}$, is about 170 Hz in the case of 1730 Pascals (13 Torr) of N_2 , and about 230 Hz in the cell without buffer gas. We conclude that there is a slightly higher relaxation rate when using the paraffin wall coating than when using the buffer gas.

Further evidence for the validity of the idea of spatial averaging comes from the behavior of $\Delta\nu_{Rb}$ versus magnetic gradient. For example, in the case of just the wall coating, $\Delta\nu_{Rb} = 280$ Hz with a gradient voltage of 1.2 volts and 260 Hz with no magnetic gradient. For the buffer gas case--at the same level of $P_{\mu\lambda}$ of 50 dB--the values are 850 Hz and 230 Hz. Still further evidence comes from the asymmetry of the line. For the buffer gas case, at 1.2 volts gradient voltage, the low frequency side of the line is 220 Hz wide and the high frequency side is 630 Hz. On the other hand, without buffer gas, the two sides differ by only 3 Hz, which is less than the precision of the linewidth measurement.

Theoretical Results

The theoretical model (based on the buffer gas case) assumes that the Rb^{87} atoms are fixed in space and that their resonant frequency depends upon their position within the cell. In the experiment, the buffer gas produces the immobility, with the intentionally applied magnetic gradient, plus the spatially changing light shift producing the frequency gradient. Figures 6 and 7 show a comparison between the theory and the data. In these figures, V_g is the voltage applied to the gradient coils; β is the microwave field intensity; K is a constant; $\delta\nu_{Rb}$ is the change in frequency between the measured (or calculated) value of ν_{Rb} and its value at $V_g = 0$ when the minimum value of microwave field is applied.

The equations used in the present calculations are based upon earlier work done by one of us (JV) and others.^{3,4,5} The values of some of the parameters that appear in the equations were determined from our or others' measurements. However, the value of pumping light intensity, I_0 , used in computing figures 6 and 7 was obtained by fitting to the data. Approximate values of I_0 , with which to begin, were obtained from reference 4.

In our calculation we assumed a gaussian optical absorption line and that, at the input end of the cell, I_0 also had a gaussian distribution.

Because the pumping light is strongly absorbed as it traverses the cell, the light shift varies rapidly along the length of the cell (see figure 8). Based on a measured average light shift of 35 Hz we estimate a light shift of 100 Hz at the entrance to the cell. Then, by adjusting the offset between the centers of the pumping and absorption lines, we attempted to get agreement with the data for no magnetic gradient ($V_g = 0.0$ of figure 6). The calculated values--at $P_{\mu\lambda} = 20$ dB, were typically too small by a factor of 2 or greater. With the probable asymmetry of the spectrum of the pumping light, it does not seem surprising to us that the agreement is poor when the gradient is due primarily to the light shift.

To perform the calculation (since the diameter of the cell is small compared to the diameter of the cavity) we assume that there is no variation of I_0 , or β , (or of the atom's frequency) across the cell, i.e., at right angles to the axis of the cell. Along the axis we use the distribution for β according to the known mode in the cavity. (In reference 1, the Q of the cavity and the cavity configuration were such that β was inadequately known for useful calculations.)

The amplitudes of a discrete (Gaussian-Hermite) spectrum of pumping light frequencies satisfy a system of first-order differential equations in the axial coordinate, Z . These were solved numerically by a Runge-Kutta method. The center of the dip in the amplitude distribution is the system frequency, ν_{Rb} .

In the measurement process we actually measure a dispersion curve rather than an absorption curve. Thus, the measured linewidth, $\Delta\nu_{Rb}$, is the width between the two dispersion peaks. To make the theoretical procedure compatible with the measurement, the first derivative is taken of the theoretical absorption curve and a theoretical $\Delta\nu_{Rb}$ obtained from the resulting dispersion curve.

On the average, the agreement of the theory with the data is sufficiently good to reinforce our belief that the two basic assumptions of the model are correct. On the other hand, there is sufficient uncertainty about the values of the experimental parameters that further attempts to fit the data presented here do not seem warranted.

Additional Thoughts On The Use of Wall Coatings

In the work reported in reference 1 we found that a change in $P_{\mu\lambda}$ of 0.4 dB about the operation

point caused a fractional change in ν_{Rb} of about 1×10^{-11} . The present work shows that, for strong gradients, there is a reduction in the $P_{\mu\lambda}$ dependence by a factor of about 100 due to the use of the wall coating. We presume that (in first order) this factor also holds at weak gradients. (Our theoretical model can address itself to this question and we are proceeding to do this. A new experimental setup is being prepared which should have measurement precision of a few parts in 10^{13} .)

Some of the major questions that need to be answered with regard to wall coatings are:

1. Will the frequency shift due to the coating be sufficiently stable (say one part in 10^{12} or better) over periods of many months?

2. Will its temperature dependence be sufficiently small?

3. If a material can be found which satisfies items 1 and 2, is its use commercially feasible?

Despite these uncertainties, the use of a wall coating has made a very large reduction in a major instability. Further studies seem warranted to determine if a significantly improved Rb standard could be developed based on a wall-coated cell.

Acknowledgments

This work was supported in part by contract SMS-80218 from the Space and Missiles Systems Organization of the U.S. Air Force, the Natural Sciences and Engineering Research Council of Canada and the Department of Education of the Province of Quebec. The authors would also like to thank Dr. Peter Bender of JILA and Dr. David Wineland of NBS for discussions regarding the data and its implications. One of us (AR) would also like to thank Mr. David Allan of NBS and Dr. Helmut Hellwig (now of Frequency & Time Systems, Inc.) for their continued interest and support.

References

1. A. Risley and G. Busca, "Effect of line inhomogeneity on the frequency of passive Rb^{87} frequency standards," Proc. 32nd Ann. Symp. on Freq. Control, pp. 506-513 (1978).
2. A. Brisson, J. Vanier, and A. Risley (unpublished).
3. Jacques Vanier, "Relaxation in rubidium-87 and the rubidium maser," Phys. Rev., Vol. 168, p. 129.
4. G. Busca, M. Tetu, and J. Vanier, "Light shift and light broadening in the ^{87}Rb maser," Can. J. Phys., Vol. 51, No. 13, July 1, 1973, pp. 1379-1387.
5. Gilles Missout and Jacques Vanier, "Some aspects of the theory of passive rubidium frequency standards," Can. J. Phys., Vol. 53, 1975, pp. 1030-1043.

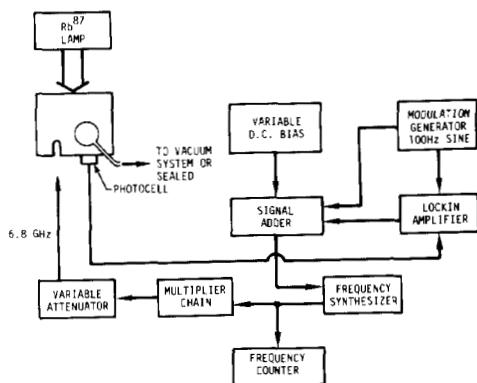


Figure 1. A schematic of the measurement system.

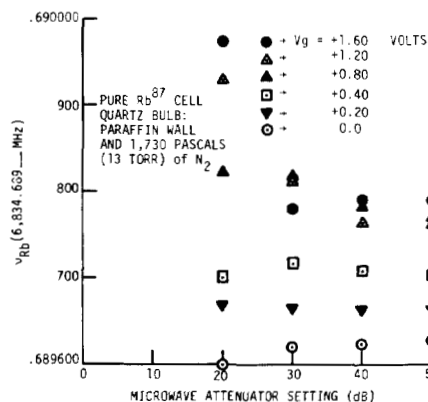


Figure 2. The output frequency, ν_{Rb} , versus applied microwave power on a cell filled with 1730 Pascals (13 Torr) of N_2 . Minimum microwave power corresponds to an attenuator setting of 50 dB. The voltage applied to the gradient coils is the parameter. A voltage, V_g , of 1.6 volts applied to the gradient coils causes a frequency change across the cell of about 2,500 Hz.

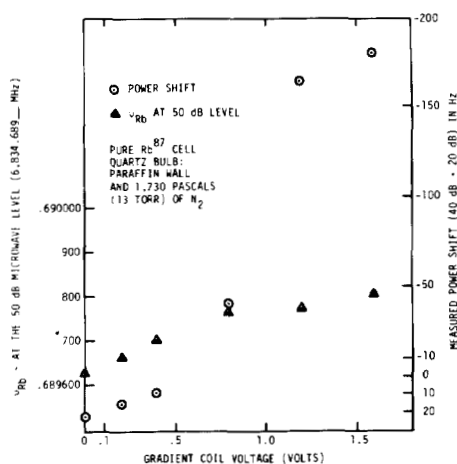


Figure 3. The data was taken on the same cell as used in figure 2. The right hand ordinate represents a frequency change due to a 20 dB change in microwave power, $P_{\mu\lambda}$. The abscissa is the voltage applied to the gradient coils and is a measure of the frequency gradient across the cell. The left hand ordinate is the output frequency at the $P_{\mu\lambda} = 50$ dB level.

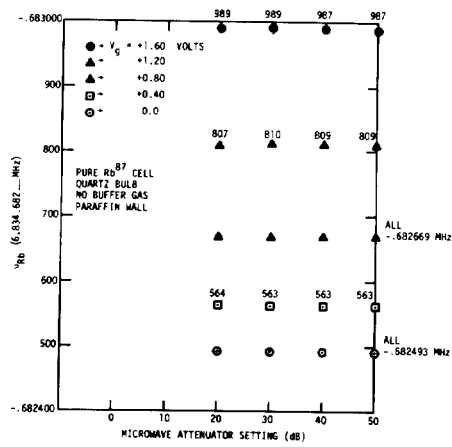


Figure 4. Same as for figure 2 except that the cell wall is coated with paraffin and the cell was kept under vacuum.

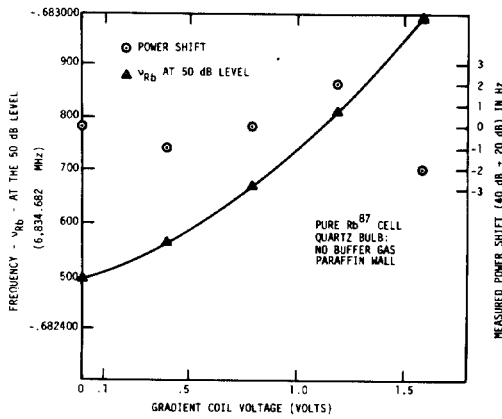


Figure 5. Same cell as for figure 4. The two ordinates and the abscissa are the same as for figure 3.

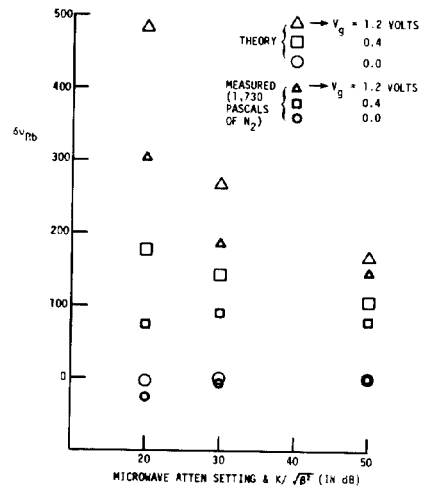


Figure 6. The theoretically obtained frequency change, $\delta\nu_{Rb}$, versus $P_{\mu\lambda}$. Also shown for comparison is some of the data of figure 2 (expressed as a frequency change).

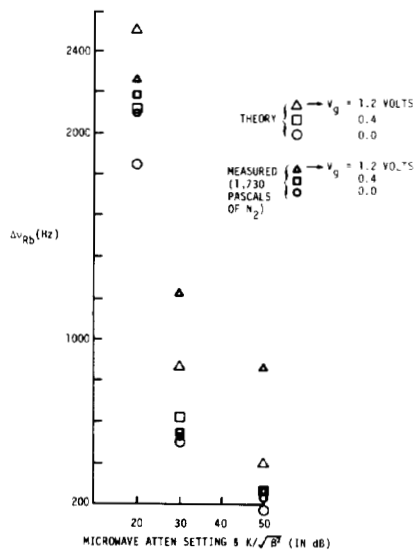


Figure 7. The theoretically obtained linewidth, $\Delta\nu_{Rb}$, versus $P_{\mu\lambda}$. The data shown corresponds to the same cell as in figures 2 and 3.

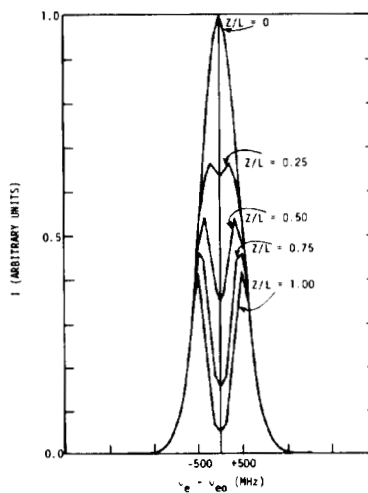


Figure 8. Calculated (theoretical) pumping light distribution, I , at several planes along the cell axis. The total length of the cell is L and Z is measured from the end of the cell where the light enters. The center of the distribution, at $Z = 0$, is at the frequency ν_{eo} .